

The angular reflectance of single-layer gradient refractive-index films

M. J. Minot

Corning Glass Works, Corning, New York 14830

(Received 22 February 1977)

Normal incidence measurements of single-layer gradient refractive-index antireflection films, produced by a chemical etch-leach process on glass sensitized by a phase-separating heat treatment, indicate very low reflection over a broad wavelength regime, 0.35–2.5 μm . First-surface measurements of the reflectance of the gradient index films have now been made, in the visible regime, at off-normal incidence (to 70°) using polarized light. These measurements show that significant reflection reduction is obtained even at high angles of incidence—5.7% reflectance from the filmed glass at 70° compared to 16.4% for the unfilmed glass. Furthermore, although the films exhibit a weak wavelength dependence at high angles, they continue to be effective over a broad spectral region. The optical properties observed are in good agreement with computations based on a gradient refractive-index film with a step at the air-film interface. The optical properties of the film offer considerable advantage over conventional interference films in many applications.

Recently, we reported the preparation of single-layer antireflection films which effectively eliminate reflections in the wavelength regime 0.35–2.5 μm .¹ The reflectance measured at near normal incidence (two surfaces) is effectively reduced from ~8% to < 1/2% over the entire visible and near-infrared regime. The films consist of a porous skeletal layer made up largely of silica produced by an etch-leach process applied to glass sensitized by a phase-separating heat treatment. The porous nature of the films leads to an effective refractive index considerably lower than ordinarily expected for a condensed film of silica. The properties of the films indicate a gradient refractive index which gets progressively steeper (Δn increases) depending on the film-forming parameters.

First-surface measurements of the reflectance properties of the gradient films have been investigated in the visible regime, as a function of the incident angle, using polarized light. For each angle, wavelength-dependent measurements were made for a mirror of aluminum evaporated on glass; ground and polished Corning Glass Works Code No. 7740 glass with no antireflection film, and Corning Glass Works Code No. 7740 with the gradient-type antireflection film. The gradient antireflection films were applied to the glass using phase-separation and film-forming techniques described in Ref. 1. Second-surface reflection effects, from both sample types, were effectively eliminated by spray painting the back surface with Krylon ultraflat black 1602-type paint.² Measurements were done on a Cary 14 spectrophotometer modified to accept a Harrick Model No. VRA-CR center-focus angular reflectance attachment.³ Polaroid Type HNP'B polarizers were used in both the sample and reference beam. The Harrick angular reflectance attachment was inserted into the sample chamber of the Cary 14, altering the optical path length without compensation in the reference beam. The measurements were not absolute and must be standardized against the spectra of well-defined materials (aluminum films in the present experiments).

CORRECTION OF EXPERIMENTAL DATA

Experimental data were corrected by comparing the measured reflectance spectra for an aluminum film to the theoretical reflectance spectra computed at various

angles on the basis of known optical constants. König gives the reflection of light at a dielectric-metal interface as follows⁴:

$$R_s = \frac{a^2 + b^2 - 2a \cos i + \cos^2 i}{a^2 + b^2 + 2a \cos i + \cos^2 i},$$

$$R_p = R_s \frac{a^2 + b^2 - 2a \sin i \tan i + \sin^2 i \tan^2 i}{a^2 + b^2 + 2a \sin i \tan i + \sin^2 i \tan^2 i},$$

and

$$\bar{R} = \frac{1}{2}(R_s + R_p),$$

where

$$a^2 = (1/2n_0^2) \{ [(n^2 - K^2 - n_0^2 \sin^2 i)^2 + 4n^2 K^2]^{1/2} + n^2 - K^2 - n_0^2 \sin^2 i \},$$

$$b^2 = (1/2n_0^2) \{ [(n^2 - K^2 - n_0^2 \sin^2 i)^2 + 4n^2 K^2]^{1/2} - n^2 + K^2 + n_0^2 \sin^2 i \}.$$

S and P designate the two planes of polarization, i is the angle of incidence, n_0 is the index of refraction of the dielectric (air), while n and K are the optical constants of the aluminum at various wavelengths. Figure 1 is a

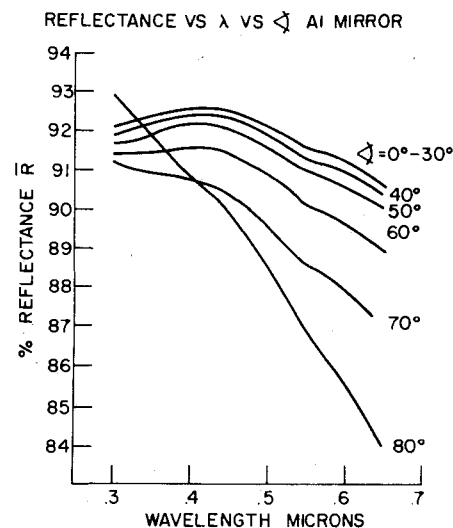


FIG. 1. Computed reflectance for an aluminum mirror as a function of angle and wavelength. These curves were computed on the basis of optical constants listed in Table I.

TABLE I. Optical constants of pure aluminum thin films (Ref. 5).

$\lambda(\mu)$	η	K
0.300	0.25	3.33
0.340	0.31	3.80
0.380	0.37	4.25
0.436	0.47	4.84
0.492	0.64	5.50
0.546	0.82	5.99
0.578	0.93	6.33
0.650	1.30	7.11

plot of the calculated reflectance versus wavelength versus angle of incidence for an Al mirror using the optical constants listed in Table I.⁵ The reflectance passes through a minimum for any particular wavelength as the incident angle is increased, before reaching 100% reflectance for 90° incidence. Figures 2-4 show the uncorrected experimentally determined reflectance curves for an aluminum mirror, Code No. 7740 glass with no film, and Code No. 7740 glass with the gradient index antireflection coating. A correction factor was determined by dividing the reflectance computed for an Al mirror by the reflectance determined experimentally for Al (Figs. 2-4). Corrected data were obtained by multiplying the experimentally determined reflectance values for filmed and unfiled samples by the correction factor. The data were corrected at specific wavelengths for each polarization.

Corrected experimental data, in terms of the S and P component, and the average reflectance, for both the gradient-type antireflection film, and for Code No. 7740 with no film, are summarized in Table II. The reflectance for Code No. 7740 as a function of angle is readily

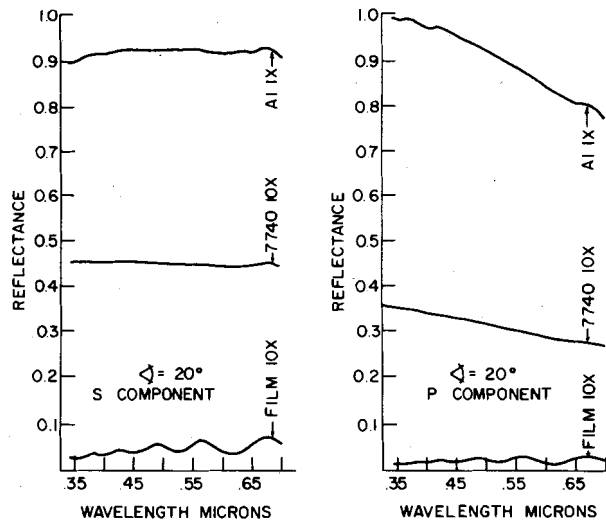


FIG. 2. Wavelength dependence of the experimental reflectance data, at an angle of 20°, for the aluminum mirror, Corning Glass Works (CGW) Code No. 7740 glass, and CGW Code No. 7740 glass coated with the gradient index antireflection film. Data for both S and P components are shown. A scale expansion of 1× or 10× is used as indicated.

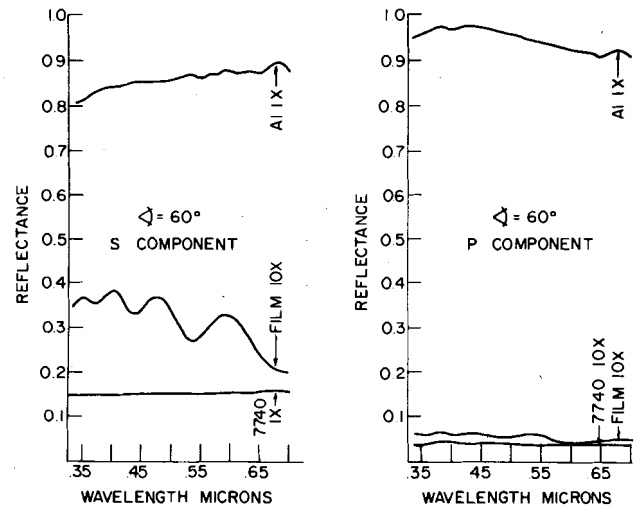


FIG. 3. Wavelength dependence of the experimental reflectance data, at an angle of 60°, for the aluminum mirror, CGW Code No. 7740 glass, and CGW Code No. 7740 glass coated with the gradient index antireflection film. Data for both S and P components are shown. A scale expansion of 1× or 10× is used as indicated.

computed using the Fresnel equations and the known refractive index 1.474. The computed reflectance as a function of angle for Code No. 7740 with no film is shown in Table III. These values, which are independent of wavelength, can be compared to the measured values listed in Table II. This comparison gives an indication of the fidelity of the measurements. Figure 5 is a plot of the corrected average reflectance (\bar{R} of Table II) versus wavelength for the films and unfiled samples at selected wavelengths. Figure 6 shows the reflectance at 5000 Å versus angle for the filmed and unfiled samples.

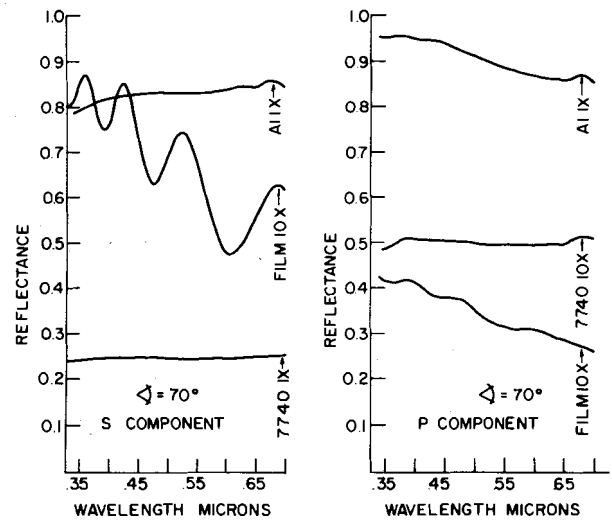


FIG. 4. Wavelength dependence of the experimental reflectance data, at an angle of 70°, for the aluminum mirror, CGW Code No. 7740 glass, and CGW Code No. 7740 glass coated with the gradient index antireflection film. Data for both S and P components are shown. A scale expansion of 1× or 10× is used as indicated.

TABLE II. Corrected reflectance of Code No. 7740 glass with and without gradient index antireflection film as a function of wavelength and angle of incidence.

λ	S polarization		P polarization		\bar{R} 7740	\bar{R} film
	7740	film	7740	film		
Angle = 20°						
3500	4.67	0.31	3.27	0.16	3.97	0.24
4000	4.58	0.36	3.20	0.17	3.89	0.27
4500	4.53	0.39	3.16	0.19	3.85	0.29
5000	3.99	0.51	3.17	0.25	3.58	0.38
5500	4.46	0.60	3.09	0.34	3.78	0.47
6000	4.42	0.42	3.07	0.19	3.75	0.31
6500	4.39	0.60	3.07	0.33	3.73	0.47
7000	4.43	0.61	3.05	0.24	3.74	0.43
Angle = 30°						
3500	5.85	0.37	2.49	0.14	4.17	0.26
4000	5.79	0.49	2.43	0.19	4.11	0.34
4500	5.68	0.56	2.39	0.23	4.04	0.40
5000	5.63	0.48	2.37	0.16	4.00	0.32
5500	5.64	0.54	2.32	0.25	3.98	0.40
6000	5.52	0.53	2.30	0.18	3.91	0.36
6500	5.51	0.65	2.30	0.29	3.91	0.47
7000	5.43	0.36	2.26	0.10	3.85	0.23
Angle = 40°						
3500	7.79	0.84	1.33	0.05	4.56	0.45
4000	7.65	0.93	1.32	0.05	4.49	0.49
4500	7.78	1.02	1.28	0.06	4.53	0.54
5000	7.50	1.37	1.24	0.09	4.37	0.73
5500	7.44	0.92	1.22	0.0095	4.33	0.46
6000	7.39	1.38	1.20	0.10	4.30	0.74
6500	7.41	0.81	1.19	0.01	4.30	0.41
7000	7.37	0.95	1.20	0.05	4.29	0.50
Angle 50°						
3500	10.67	1.96	0.34	0	5.51	0.98
4000	10.46	2.22	0.32	0	5.39	1.11
4500	10.28	2.34	0.29	0	5.29	1.17
5000	10.24	1.73	0.29	0	5.27	0.87
5500	10.24	2.34	0.28	0	5.26	1.17
6000	10.38	1.36	0.26	0	5.32	0.68
6500	10.43	1.87	0.26	0	5.35	0.94
7000	10.54	1.89	0.27	0	5.41	0.95
Angle 60°						
3500	17.83	4.31	0.35	0.54	9.09	2.43
4000	17.43	4.36	0.40	0.56	8.92	2.46
4500	17.12	3.77	0.36	0.55	8.74	2.16
5000	17.02	3.69	0.36	0.49	8.69	2.09
5500	16.88	3.11	0.36	0.52	8.62	1.82
6000	16.57	3.54	0.36	0.39	8.47	1.97
6500	16.64	2.53	0.37	0.44	8.51	1.49
7000	17.00	2.15	0.36	0.45	8.68	1.30
Angle 70°						
3500	29.42	10.17	4.34	3.74	16.88	6.96
4000	28.95	9.08	4.88	3.68	16.92	6.38
4500	28.55	8.58	4.48	3.37	16.52	5.98
5000	28.40	8.16	4.39	3.17	16.40	5.67
5500	28.14	7.97	4.46	2.80	16.30	5.39
6000	28.10	5.52	4.47	2.80	16.29	4.16
6500	28.09	6.31	4.47	2.56	16.28	4.42
7000	28.38	6.95	4.50	2.27	16.44	4.61

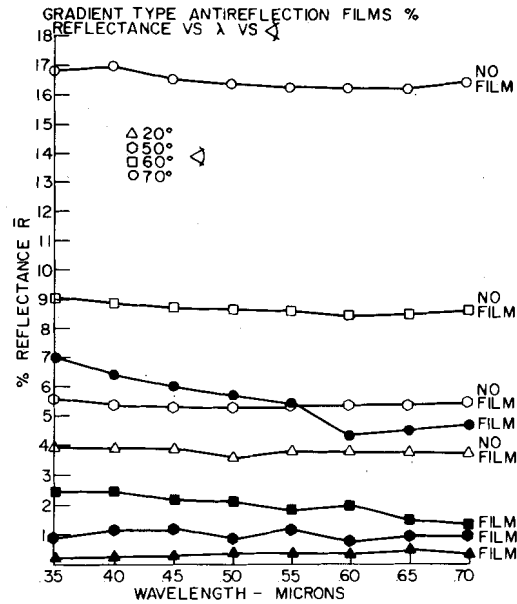


FIG. 5. Plot of corrected average reflectance [$\bar{R} = \frac{1}{2}(R_s + R_p)$] vs wavelength vs angle for CGW Code No. 7740 glass (no film) and CGW Code No. 7740 coated with the gradient-type anti-reflection film.

Inspection of Figs. 5 and 6 indicates that the gradient antireflection film provides a significant low-reflection advantage at relatively high angles. For example, at 70° incidence, the reflectance of the porous antireflection film at 5000 Å is 5.7% compared to 16.4% for the uncoated glass. Under similar conditions, a conventional MgF₂ quarter-wave film (centered at 5000 Å, $\eta = 1.38$, on glass $\eta = 1.474$), would reflect 13.3%. The reflection of the gradient antireflection films is largely insensitive to wavelength. Close inspection of the data reveals that, for low angles of incidence, the reflection increases slightly with wavelength. Above 40° incidence, the reflection slowly decreases at longer wavelengths. This is particularly apparent at 70° incidence where the reflection drops approximately 2% between 0.35 and 0.7 μm . Finally, inspection of the uncorrected experimental data, Figs. 2-4, reveals periodic oscillation of the reflection as a function of wavelength. The amplitude of these oscillations increases at higher angles, becoming as great as $\pm 0.75\%$ at 70° and 5000 Å. This detail is lost in Fig. 5, where the data were corrected point by point at 0.5 μm intervals.

TABLE III. Computed reflectance versus angle.

Angle κ	Code No. 7740		$\eta = 1.474$
	R_p (%)	R_s (%)	\bar{R} (%) = $\frac{1}{2}(R_s + R_p)$
20°	3.06	4.33	3.70
30°	2.29	5.34	3.82
40°	1.28	7.17	4.22
50°	0.27	10.51	5.39
60°	0.22	16.75	8.48
70°	4.37	28.84	16.61
90°	1	1	1

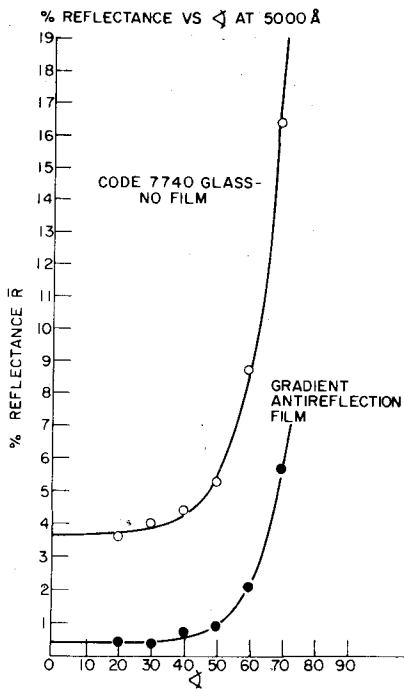


FIG. 6. Comparison of the reflectance as a function of angle, at $\lambda = 5000 \text{ \AA}$, of CGW Code No. 7740 glass with and without the gradient index antireflection film.

COMPARISON OF EXPERIMENTAL DATA WITH CALCULATED CURVES

The experimentally observed reflectance curves for various angles are in good qualitative agreement with curves computer generated for an assumed gradient refractive index profile "bounded" at the air-film interface. A continuously varying refractive index profile is readily approximated by a series of discrete films, such that the refractive index of each is assumed to be constant.⁶ Figure 7 is a geometrical representation of a thin inhomogeneous dielectric film whose refractive index changes linearly with film thickness. The dotted step profile, offset for ease of illustration, shows the inhomogeneous film approximated by a series of thin homogeneous films. Ten such steps are generally sufficient to approximate most gradient profiles. This approximation is particularly advantageous when used in

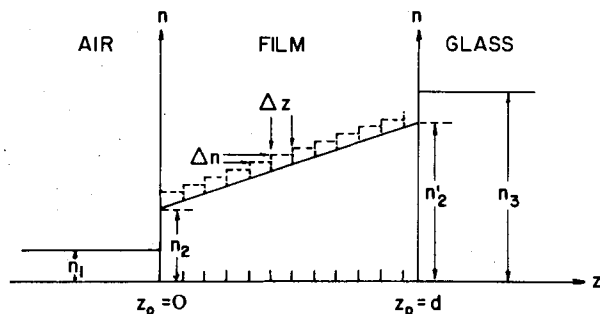


FIG. 7. Geometrical representation of a thin inhomogeneous film whose refractive index changes linearly with film thickness. The dotted step profile, offset for ease of illustration, shows the inhomogeneous film approximated by a series of thin homogeneous films.

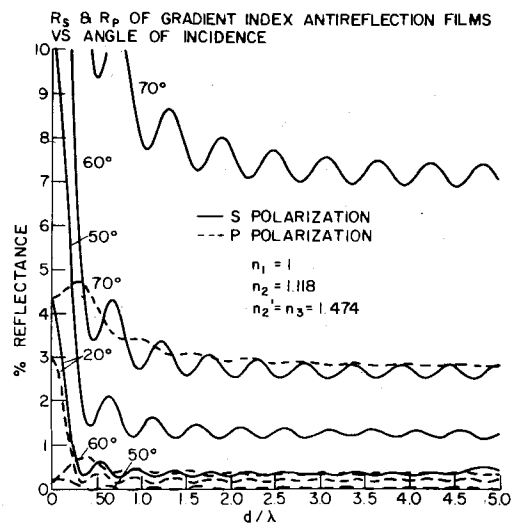


FIG. 8. Computer-calculated reflectance, for both the S and P polarization, as a function of angle, plotted against d/λ for the case of an antireflection film characterized by a linear gradient refractive-index profile where $n_1 = 1$, $n_2 = 1.118$, and $n_2' = n_3 = 1.474$.

conjunction with matrix notation. The value of the matrix approach lies in the fact that the optical behavior of the film is entirely determined by its characteristic matrix which depends on the optical constants inside the film, and is independent of the surrounding media. For the case of a gradient index film, approximated by a stack of homogeneous discrete layers, the characteristic matrix M is given as the product of the matrices of the sublayers $M_i(Z_i)$, or

$$M = \prod_{i=1}^P M_i(Z_{(i)} - Z_{(i-1)})$$

The reflection and transmission coefficients in terms of the elements m_{ij} of the characteristic matrix as well as the characteristic matrix for a discrete homogeneous film are readily available in the literature.⁷

Figure 8 shows the calculated reflectance for both the S and the P polarization as a function of angle plotted against d/λ for the case where $n_1 = 1$, $n_2 = 1.118$, $n_2' = n_3 = 1.474$, i. e., a gradient index film "bounded" by a discrete air-film interface. The transition between film and bulk glass was assumed to be continuous. A linear refractive index profile was assumed for this case. Figure 9 shows the average reflectance, $\bar{R} = \frac{1}{2}(R_s + R_p)$, plotted for the same gradient profile. These computed results can be compared to the raw experimental data, Figs. 2-4, as well as the corrected data, Figs. 5 and 6. For a given film thickness, the reflectance goes up as expected with angle of incidence. The films exhibit a weak but real periodic wavelength dependence. The amplitude of these oscillations lessens as wavelength is decreased relative to film thickness, but increases as the angle of incidence is increased. These periodic oscillations are analogous to the periodic maxima and minima observed for a single-layer discrete homogeneous thin film. In the case of the discrete homogeneous thin film, the amplitude of the oscillations does not diminish as d/λ increases, i. e., all maxima correspond to the Fres-

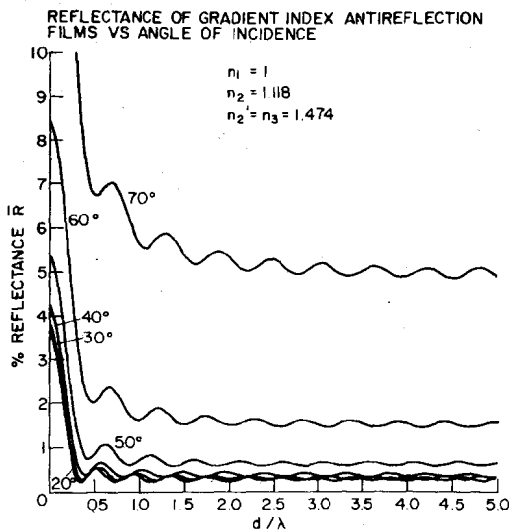


FIG. 9. Computer-calculated average reflectance $\bar{R} = \frac{1}{2}(R_s + R_p)$ as a function of angle, plotted against d/λ for the same film as shown in Fig. 8.

nel reflectance of the uncoated glass. In both cases, the position of the minima shifts to shorter wavelengths as angle is increased. The computed results indicate that in the long-wavelength limit ($d/\lambda \rightarrow 0$), the reflectance increases, approaching the reflectance of the uncoated glass at the given angle (compare to Table III). Indeed the experimental results, at low angles, indicate a slight increase of reflectance at longer wavelengths. At the higher angles of incidence, however, an unexpected decrease of reflectance is observed at longer wavelengths. The unexplained decrease in reflectance observed at high angles and long wavelength might be related to specific details of the actual refractive index profile, or alternatively to λ^{-4} scattering phenomena.

DISCUSSION

Single-layer gradient refractive-index antireflection films, produced by a chemical etch-leach process on glass sensitized by a phase-separating heat treatment exhibit very low reflection over a broad wavelength regime, 0.35–2.5 μm , at normal incidence. The reflection properties of these gradient index films have now been measured in the visible regime at off-normal incidence (to 70°) using polarized light. Measurements indicate that the gradient index films provide considerable low-reflection effects at angles where conventional homogeneous discrete thin films have lost their utility. The reflectance of the gradient index films exhibits a real but very small wavelength dependence. The reflectance differences between wavelength-dependent maxima and minima are small at 70° and negligible at lower angles, so that the films continue to be very effective over broad

regions of the spectra. Although our high-angle measurements have not been extended beyond 0.7 μm , the theory suggests that low-reflection effects can be expected well into the infrared as is observed for normal incidence.

The measured optical properties of the films are in good agreement with computations based on a film with a linear refractive index profile with a step at the air-film interface. The assumption of a step at the air-film interface results in a considerably better fit to the experimental data than similar computations assuming an "unbounded" profile, i. e., no step at the air-film interface, or to computations assuming a step at both the air-film, and the film-glass interface. The assumption of a profile with a step at both the air-film and film-glass interface leads to reflectance values characterized by periodic wavelength-dependent oscillations of considerably greater magnitude than is observed for these films experimentally. The assumption of an unbounded profile is physically untenable and leads to considerably lower reflectance values than are observed experimentally. The computed optical properties, however, appear largely insensitive to details of the refractive-index profile, i. e., linear versus hyperbolic versus exponential, and we cannot expect to infer the shape of the profile from the computations. Indeed, based on our understanding of etching phenomena, it is unlikely that the profile is linear.

The low broadband reflectance, and the lack of sensitivity to angle of incidence characteristic of these films should prove very advantageous in a number of applications, such as, for example, solar energy. Preliminary outdoor weather testing of these films indicates very little loss of transmission with exposure.

ACKNOWLEDGMENT

The author wishes to acknowledge Dr. Michael Teter, Corning Glass Works, for his assistance in setting up the computer computations.

¹M. J. Minot, *J. Opt. Soc. Am.* 66, 515–519 (1976).

²Krylon® Paint, Borden, Inc., Columbus, Ohio.

³Harrick Scientific Corp., Ossining, N. Y.

⁴W. Konig, *Handbuch der Physik*, Vol. 20 (Springer, Berlin, 1928), p. 66.

⁵G. Hass and J. E. Waylonis, *J. Opt. Soc. Am.* 50, 1133 (1960).

⁶R. Jacobsson, *Progress in Optics V*, edited by E. Wolf (North-Holland, Amsterdam, 1966), p. 249.

⁷M. Born and E. Wolf, *Principles of Optics* (Pergamon, New York, 1975), pp. 55–61.